Supporting Information for

General Facet-Controlled Synthesis of Single-Crystalline {010}-Oriented $LiMPO_4$ (M = Mn, Fe, Co) Nanosheets

Lele Peng,[†,§] Xiao Zhang,[†,§] Zhiwei Fang,[†,§] Yue Zhu,[†] Yujun Xie,[‡] Judy Cha,[‡] Guihua Yu[,†]*

[†] Materials Science and Engineering Program and Department of Mechanical Engineering, The University of Texas at Austin, Austin, Texas 78712, United States

[‡] Department of Mechanical Engineering and Materials Science, Yale University, New Haven, Connecticut 06520, United States.

[§] These authors contributed equally to this work.

**Correspondence should be addressed: ghyu@austin.utexas.edu (G.Y.)*

EXPERIMENTAL METHODS

Preparation of $LiMPO_4$ nanosheets. The preparation of $LiMPO_4$ nanosheets involves the synthesis of $LiMPO_4$ nanosheet assembled powders and exfoliation of the powders into thin nanosheets. The powders were obtained in a solvothermal reaction with diethylene glycol as solvent and Poly(vinylpyrrolidone) (PVP) as surfactants. In a typical experiment, 1 mmol of $MnCl_2$/$FeCl_2$/$CoCl_2$, 0.5 mmol of LiAc and 50 mg PVP were dissolved in 7.5 mL diethylene glycol. To avoid the oxidation of the metal ions, the suspensions were bubbled with N_2 gas for sufficient time. 1 mmol of LiH_2PO_4 was dissolved in 0.4 mL water and the as-formed aqueous solution was drop-wisely added into the diethylene glycol with constant stirring until a homogenous suspension was formed. The suspension was thermally aged in a stainless steel autoclave at 220 °C for 20 hours. The powders were washed with water and ethanol for three times after the solvothermal treatment, and dried in a vacuum oven at 80 ˚C for overnight. The $LiMPO_4$ nanosheets can be obtained by exfoliating the as-obtained powders in ethanol in the bath sonication equipment.

Carbon coating of the $LiFePO_4$ nanosheets and fabrication of the $LiFePO_4$ nanosheets electrode. Carbon coating of the as-exfoliated $LiFePO_4$ nanosheets was achieved by annealing the $LiFePO_4$ nanosheets with sucrose in the inert atmosphere. In a typical procedure, the as-prepared $LiFePO_4$ nanosheets, sucrose (10% in weight ratio), and proper amount of deionized water were mechanically mixed in Thinky centrifugal mixer (ARE-310) for 30 min, dried in vacuum, and annealed in pure Ar atmosphere at 650 ˚C for 12 hours. The electrode was prepared by mixing the as-prepared carbon-coated $LiFePO_4$ nanosheets, Super P carbon (Timcal Graphite & Carbon), and polyvinylidene fluoride binder (Fisher Scientific) with a weight ratio of 80: 15: 5 in N-methyl-2-pyrrolidone (anhydrous, Fisher Scientific). The mixture was thoroughly mixed in Thinky centrifugal mixer to form the homogenous slurry, which was then casted on aluminum foil and dried in vacuum at 115 °C for 12 hrs.

Cell assembly. The electrochemical performance was evaluated with a standard CR2032 coin cell using metallic lithium as the anode, Celgard 2500 as the separator, and $LiPF_6$ in 1:1 ethylene carbonate and diethyl carbonate (BASF Corp.) as the electrolyte.

Characterizations. Powder X-ray diffraction (XRD) patterns of the as-synthesized $LMPO_4$ nanosheets were performed on the Miniflex equipped with Cu Kα radiation. Scanning electron microscopy (SEM) and transmission electron (TEM) of the $LMPO_4$ nanosheets were characterized by Hitachi S-5500 and JEOL (2010F), respectively. FT-IR and Raman spectrums were performed on Thermal Scientific FT-IR spectrometer (NicoletTM iSTM5) and Renishaw Raman system equipped with a 633 nm argon ion laser, respectively. Electrochemical characterization was performed on LANHE battery cycler (CT2001A) and Bio-logic potentiostat (VMP3) equipped with impedance modules.

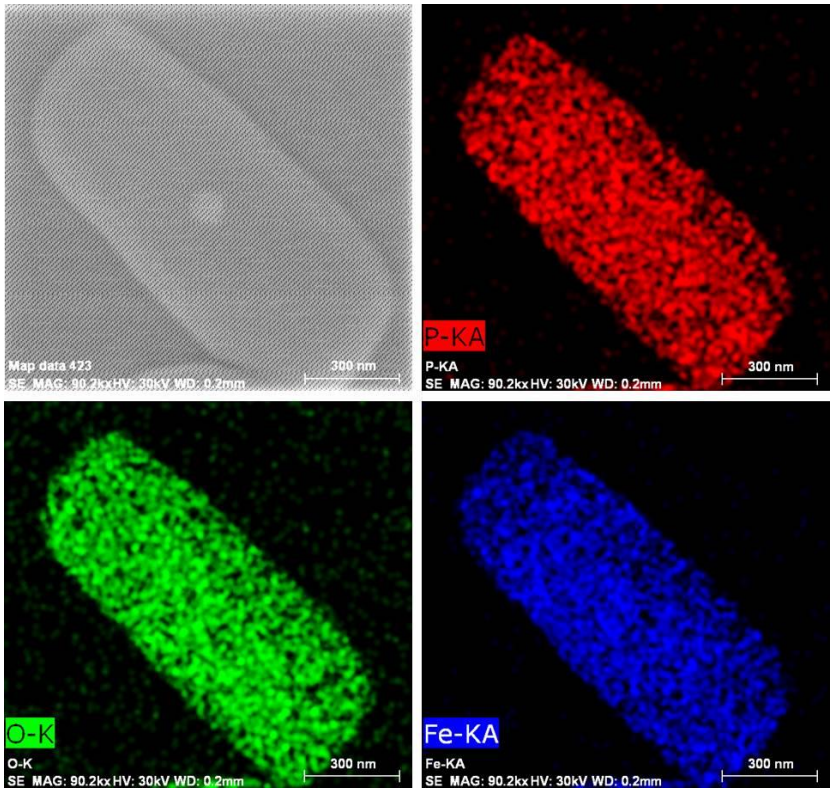

Figure S1. EDX mapping of P, O and Fe elements of $LiFePO_4$ nanosheets.

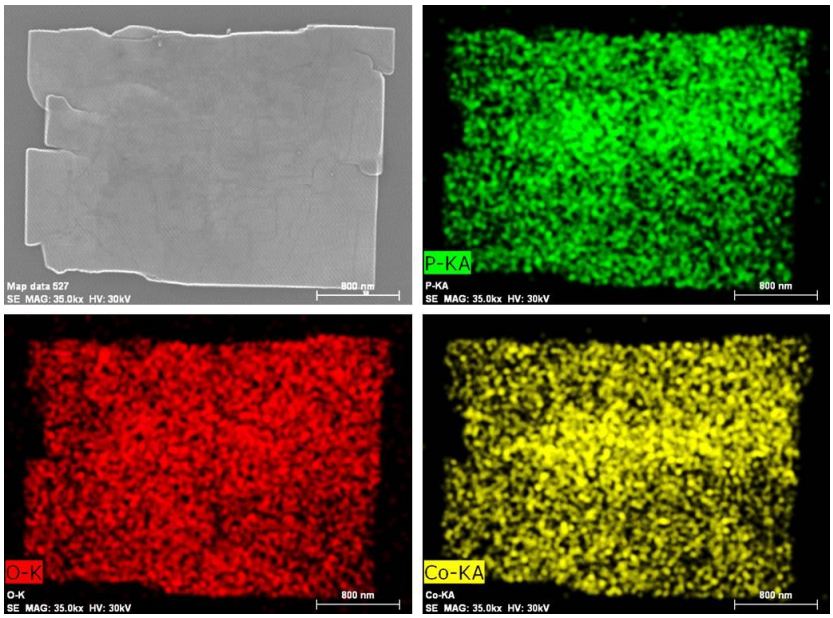

Figure S2. EDX mapping of P, O and Co elements of $LiCoPO_4$ nanosheets.

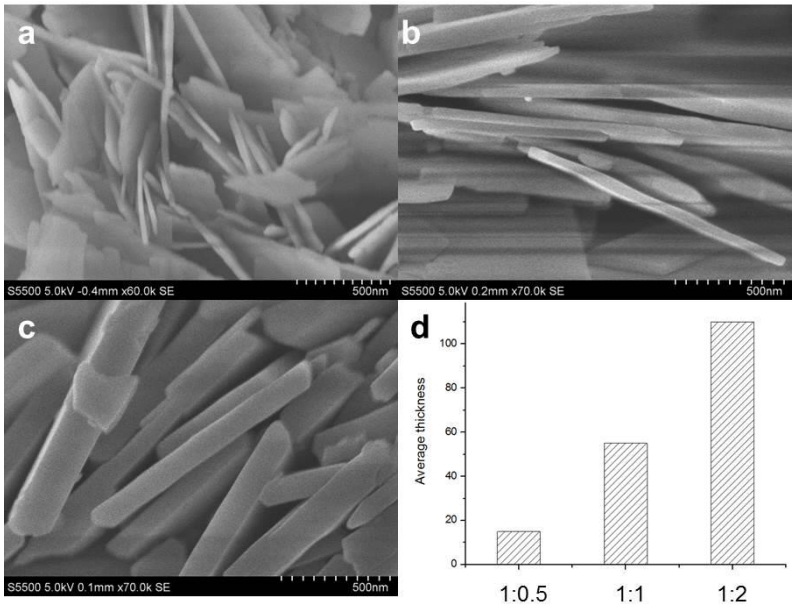

Figure S3. SEM images of the $LiFePO_4$ nanosheets obtained with the molar ratio of Fe:P of 1:0.5 (a), 1:1 (b) and 1:2 (c). (d) Thickness distribution of the $LiFePO_4$ nanosheets obtained with the molar ratio of Fe:P of 1:0.5, 1:1 and 1:2.

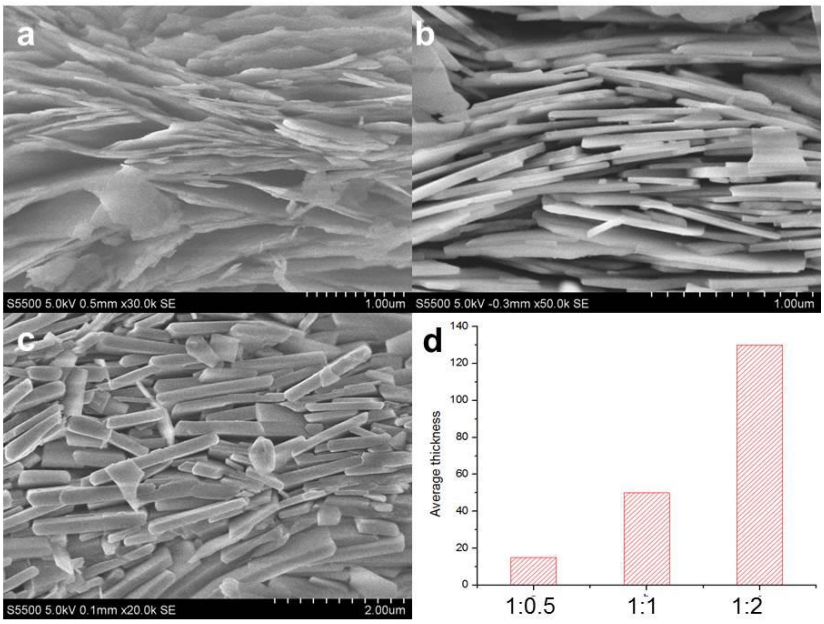

Figure S4. SEM images of the $LiCoPO_4$ nanosheets obtained with the molar ratio of Co:P of 1:0.5 (a), 1:1 (b) and 1:2 (c). (d) Thickness distribution of the $LiCoPO_4$ nanosheets obtained with the molar ratio of Co:P of 1:0.5, 1:1 and 1:2.

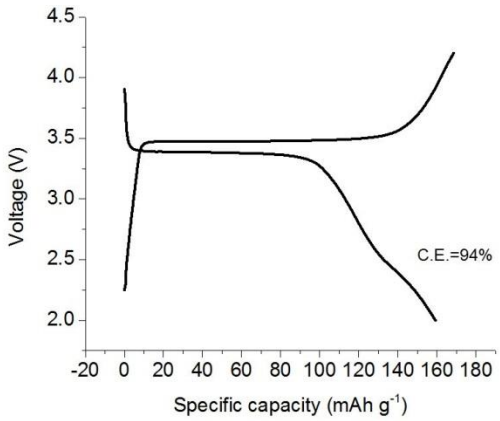

Figure S5. Charge-discharge curve of the $LiFePO_4$ nanosheet electrodes in the first cycle at 0.5 C.

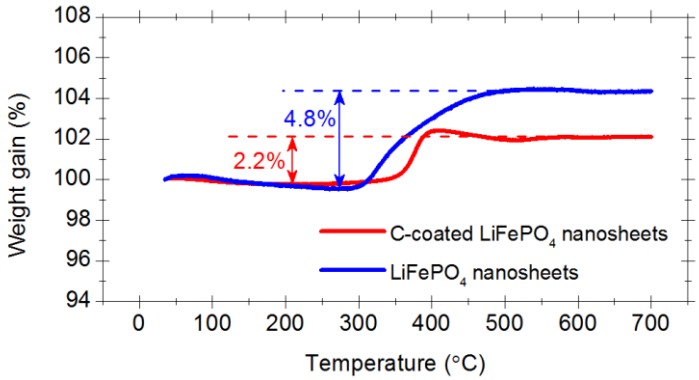

Figure S6. Thermal gravimetric analysis (TGA) of the carbon-coated $LiFePO_4$ nanosheets and pure $LiFePO_4$ nanosheets.

Both the $LiFePO_4$ nanosheets with and without carbon coating show a very slight weight loss at the temperature around 100 ˚C, and exhibit a weight gain when the temperature approaches 300 ˚C. This weight gain is due to the oxidation of $LiFePO_4$ to $Li_3Fe_2(PO_4)_3$ and Fe_2O_3. The oxidation process of carbon coated $LiFePO_4$ at the temperature range from 300 ˚C to 700 ˚C can be described as the following equation:

$$LiFePO_4/C + \frac{1}{4}O_2 + nO_2 \rightarrow \frac{1}{3}Li_3Fe_2(PO_4)_3 + \frac{1}{6}Fe_2O_3 + nCO_2$$

The TGA curve above 550 °C becomes very stable, indicating that the oxidation of $LiFePO_4$ and carbon is complete. As read from the curve, the overall weight gain of the carbon coated $LiFePO_4$ nanosheets is about 2.2%, and the weight gain of the pure $LiFePO_4$ nanosheets is 4.8%. Thus, the carbon content in the carbon coated $LiFePO_4$ nanosheets is 2.6 % in terms of the weight.

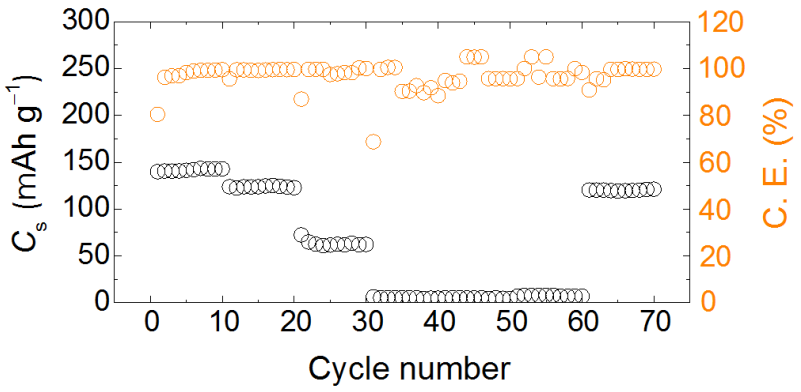

Figure S7. Rate capability and the corresponding C.E. of commercial $LiFePO_4$ powders. The reason for the unstable C.E. after the 30th cycle is because the commercial $LiFePO_4$ electrodes are not rechargeable at that high C rate.

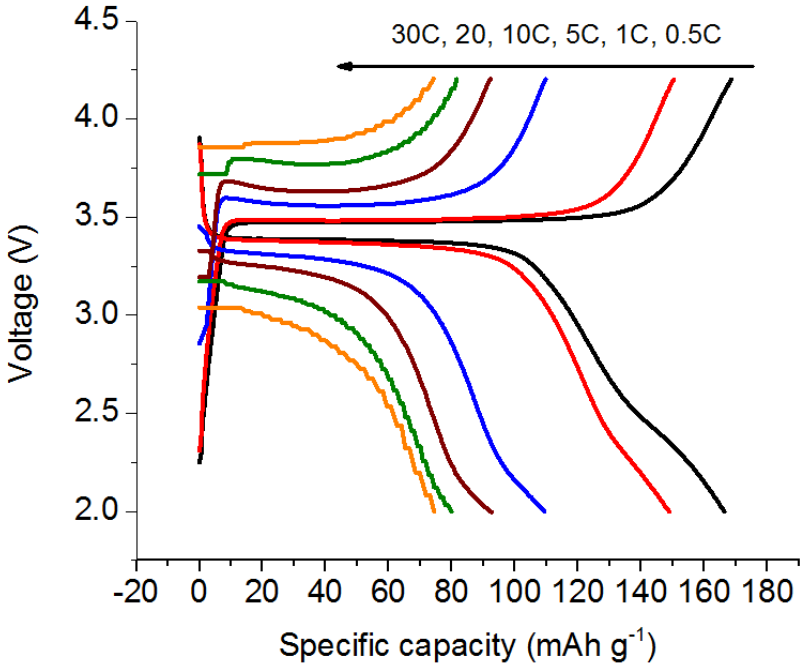

Figure S8. Charge-discharge cures of the $LiFePO_4$ nanosheets at various C rates.

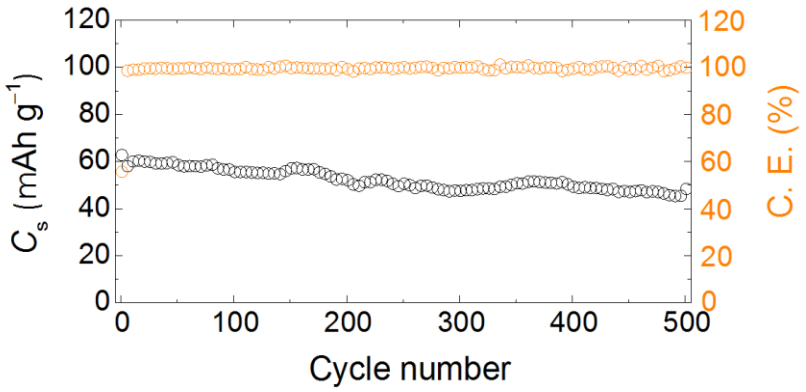

Figure S9. Cycling stability and the corresponding C.E. of commercial $LiFePO_4$ powders.

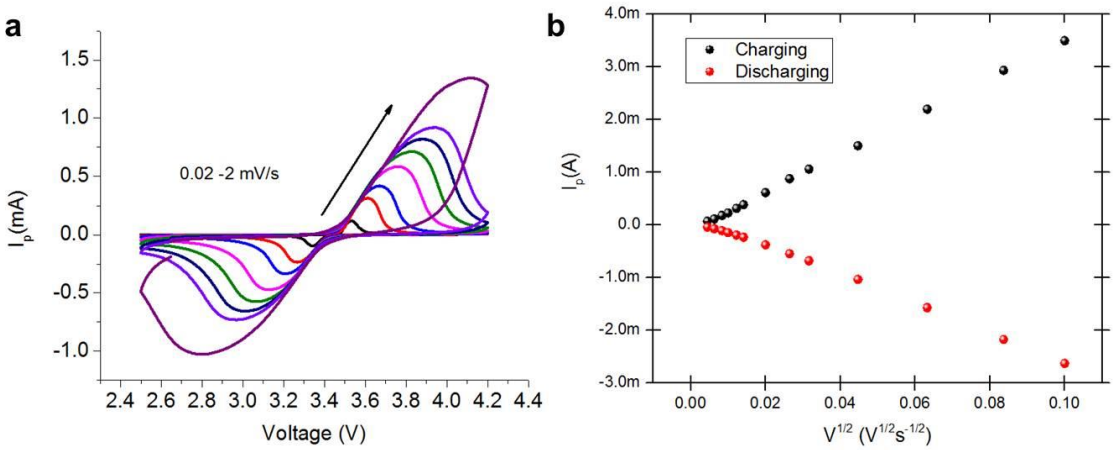

Figure S10. CV curves of the commercial $LiFePO_4$ powders at various scan rates.

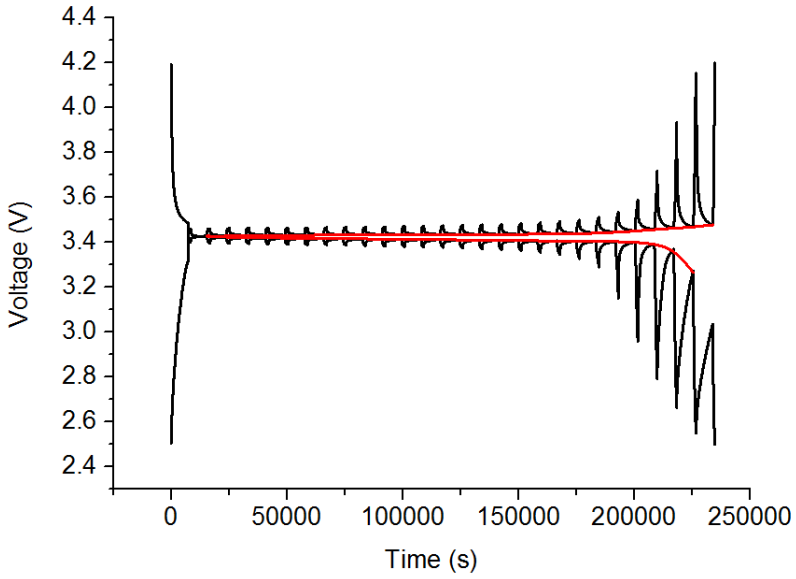

Figure S11. GITT curves and the open-circuit voltage profile of the $LiFePO_4$ nanosheets.

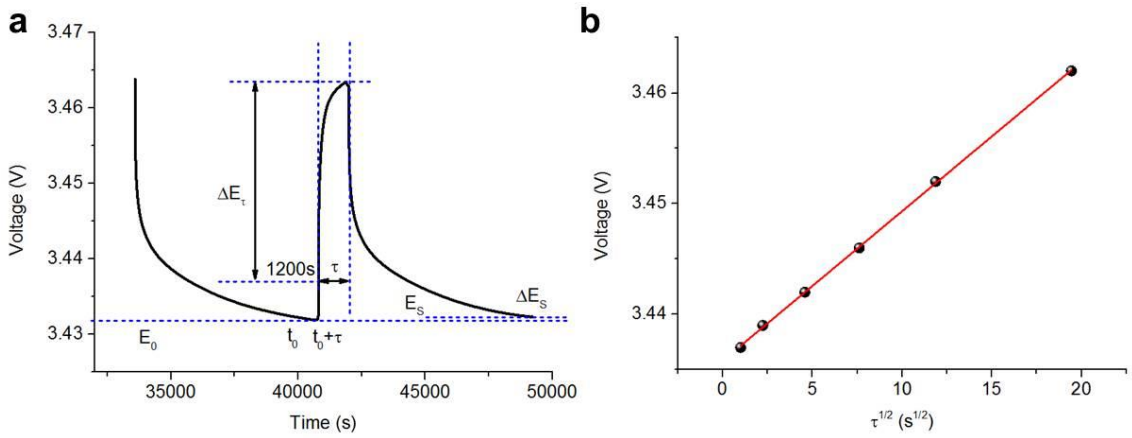

Figure S12. Real-time voltage versus time profile and the linear relationship in the GITT curve of $LiFePO_4$ nanosheet electrodes.

Materials/structures	**Rate performance**	**Cycling performance**	**Ref**
(100)-exposed $LiFePO_4$ nanoplates	146 mAh g^{-1} at 1 C 96 mAh g^{-1} at 5 C	N.A.	1
(010)-exposed $LiFePO_4$ nanoplates	135 mAh g^{-1} at 1 C 82 mAh g^{-1} at 10 C	N.A.	2
$LiFePO_4$ hexagonal nanoplates	150 mAh g^{-1} at 1 C 130 mAh g^{-1} at 5 C	N.A.	3
$LiFePO_4$ nanoplates	160 mAh g^{-1} at 0.15 C 100mAh g^{-1} at 3.45 C	155 mAh g^{-1} after 50 cycles (0.2 C)	4
$LiFePO_4$ nanoplates	125 mAh g^{-1} at 1 C 80mAh g^{-1} at 20 C	78 mAh g^{-1} after 300 cycles (20 C)	5
$LiFePO_4$ nanoplates	143 mAh g^{-1} at 0.5 C 47 mAh g^{-1} at 30 C	48 mAh g^{-1} after 50 cycles (30 C)	6
$LiFePO_4$ nanoplates	165 mAh g^{-1} at 0.1 C 140 mAh g^{-1} at 5 C	145 mAh g^{-1} after 30 cycles (1 C)	7
$LiFePO_4$ nanoplates assembled hierarchical structures	145 mAh g^{-1} at 0.2 C 48 mAh g^{-1} at 30 C	160 mAh g^{-1} after 50 cycles (0.1 C)	8
Sandwich-like $LiFePO_4$/graphene hybrid nanosheets	157 mAh g^{-1} at 1 C 115 mAh g^{-1} at 10 C	70 mAh g^{-1} after 30 cycles (20 C)	9
Hierarchical $LiFePO_4$ microplates	157 mAh g^{-1} at 1 C 82 mAh g^{-1} at 20 C	120 mAh g^{-1} after 100 cycles (5 C)	10
Monodisperse porous $LiFePO_4$ microspheres	140 mAh g^{-1} at 0.5 C 35 mAh g^{-1} at 30 C	90 mAh g^{-1} after 600 cycles (10 C)	11
Self-assembled $LiFePO_4$ nano/microspheres	155 mAh g^{-1} at 0.1 C 95 mAh g^{-1} at 5 C	120 mAh g^{-1} after 100 cycles (1 C)	12
$LiFePO_4$ hierarchically dumbbell-like microstructures	110 mAh g^{-1} at 1/30 C	117 mAh g^{-1} after 70 cycles (1/30 C)	13
$LiFePO_4$ nanoplate microspheres	150 mAh g^{-1} at 1 C 85 mAh g^{-1} at 5 C	152 mAh g^{-1} after 50 cycles (0.1 C)	14
(010)-exposed $LiFePO_4$ nanosheets	160 mAh g^{-1} at 0.5 C 80 mAh g^{-1} at 30 C	120 mAh g^{-1} after 500 cycles (5 C)	**This work**

Table S1. Comparison of the overall electrochemical performance of the $LiFePO_4$ nanosheets with other $LiFePO_4$ nanosheets/nanoplates reported in the literature.

References:

(1) Ju, S.; Peng, H.; Li, G.; Chen, K. Synthesis and Electrochemical Properties Of $LiFePO_4$ Single-Crystalline Nanoplates Dominated with bc-Planes. *Mater. Lett.* **2012**, *74*, 22-25.

(2) Ma, Z.; Shao, G.; Wang, X.; Song, J.; Wang, G.; Liu, T. Solvothermal Synthesis of $LiFePO_4$ Nanoplates with (010) Plane and the Uniform Carbon Coated on their Surface by Esterification Reaction. *Mater. Chem. Phys.* **2014**, *143*, 969-976.

(3) Gao, C.; Zhou, J.; Liu, G.; Wang, L. Microwave-Assisted Synthesis and Surface Decoration of $LiFePO_4$ Hexagonal Nanoplates for Lithium-Ion Aatteries with Excellent Electrochemical Performance. *J. Mater. Sci.* **2017**, *52*, 1590-1602.

(4) Sinha, N. N.; Munichandraiah, N. Single-Shot Preparation of Crystalline Nanoplate $LiFePO_4$ by a Simple Polyol Route. *J. Electrochem. Soc.* **2010**, *157*, A824-A829.

(5) Song, J.; Sun, B.; Liu, H.; Ma, Z.; Chen, Z.; Shao, G.; Wang, G. Enhancement of the Rate Capability of $LiFePO_4$ by a New Highly Graphitic Carbon-Coating Method. *ACS Appl. Mater. Interfaces* **2016**, *8*, 15225-15231.

(6) Saravanan, K.; Reddy, M. V.; Balaya, P.; Gong, H.; Chowdari, B. V. R.; Vittal, J. J. Storage Performance of $LiFePO_4$ Nanoplates. *J. Mater. Chem.* **2009**, *19*, 605-610.

(7) Saravanan, K.; Balaya, P.; Reddy, M. V.; Chowdari, B. V. R.; Vittal, J. J. Morphology Controlled Synthesis of $LiFePO_4$/C Nanoplates for Li-Ion Batteries. *Energy Environ. Sci.* **2010**, *3*, 457-463.

(8) Nan, C.; Lu, J.; Chen, C.; Peng, Q.; Li, Y. Solvothermal Synthesis of Lithium Iron Phosphate Nanoplates. *J. Mater. Chem.* **2011**, *21*, 9994-9996.

(9) Guo, X.; Fan, Q.; Yu, L.; Liang, J.; Ji, W.; Peng, L.; Guo, X.; Ding, W.; Chen, Y. Sandwich-Like $LiFePO_4$/Graphene Hybrid Nanosheets: In Situ Catalytic Graphitization and Their High-Rate Performance for Lithium Ion Batteries. *J. Mater. Chem. A* **2013**, *1*, 11534-11538.

(10) Zhang, J.; Lu, J.; Bian, D.; Yang, Z.; Wu, Q.; Zhang, W. Solvothermal Synthesis of Hierarchical $LiFePO_4$ Microplates with Exposed (010) Faces as Cathode Materials for Lithium Ion Batteries. *Ind. Eng. Chem. Res.* **2014**, *53*, 12209-12215.

(11) Sun, C.; Rajasekhara, S.; Goodenough, J. B.; Zhou, F. Monodisperse Porous $LiFePO_4$ Microspheres for a High Power Li-Ion Battery Cathode. *J. Am. Chem. Soc.* **2011**, *133*, 2132-2135.

(12) Su, J.; Wu, X.-L.; Yang, C.-P.; Lee, J.-S.; Kim, J.; Guo, Y.-G. Self-Assembled $LiFePO_4$/C Nano/Microspheres by Using Phytic Acid as Phosphorus Source. *J. Phys. Chem. C* **2012**, *116*, 5019-5024.

(13) Yang, H.; Wu, X.-L.; Cao, M.-H.; Guo, Y.-G. Solvothermal Synthesis of $LiFePO_4$ Hierarchically Dumbbell-Like Microstructures by Nanoplate Self-Assembly and Their Application as a Cathode Material in Lithium-Ion Batteries. *J. Phys. Chem. C* **2009**, *113*, 3345-3351.

(14) Wu, Y.; Wen, Z.; Li, J. Hierarchical Carbon-Coated $LiFePO_4$ Nanoplate Microspheres with High Electrochemical Performance for Li-Ion Batteries. *Adv. Mater.* **2011**, *23*, 1126-1129.